Revista de Osteoporosis y Metabolismo Mineral

Original

Effect of extracellular vesicles derived from hypoxia-preconditioned human mesenchymal stem cells on osteoblastogenesis and adipogenesis *in vitro*

Carolina Jiménez-Navarro[1], Bárbara Torrecillas-Baena[1,2], Marta Camacho-Cardenosa[1,2], José Manuel Quesada-Gómez[1], María Ángeles Gálvez-Moreno[1,2], Antonio Casado-Díaz[1,2,3]

[1]Instituto Maimónides de Investigación Biomédica de Córdoba (IMIBIC). Hospital Universitario Reina Sofía. Córdoba, Spain. [2]Unidad de Gestión Clínica de Endocrinología y Nutrición. Hospital Universitario Reina Sofía. Córdoba, Spain. [3]Centro de Investigación Biomédica en Red de Fragilidad y Envejecimiento Saludable (CIBERFES). Instituto de Salud Carlos III. Madrid, Spain

Abstract

Objectives: mesenchymal stem cells (MSC) are characterized by their anti-inflammatory, immunosuppressive activity, and their ability to differentiate. This makes them an interesting therapeutic tool in cell therapy and regenerative medicine. In part, the therapeutic effect of MSC is mediated by the secretion of extracellular vesicles (EV). The preconditioning of MSC in hypoxia can enhance the regenerative capacity of the secreted EV. In this context, the aim of the study was to evaluate whether EV derived from human MSC cultured in normoxic and hypoxic conditions affect the osteoblastogenesis and adipogenesis of MSC.

Material and methods: EV were isolated from MSC maintained for 48 hours in normoxic or hypoxic conditions (3 % O_2) using ultrafiltration and size exclusion chromatography. The EV were characterized by Western blot, electron microscopy, and nanoparticle tracking analysis. In MSC cultures, the effect of the EV on viability was evaluated using an MTT assay, migration was assessed with the Oris assay while differentiation into osteoblasts and adipocytes was also studied.

Results: the EV increased viability and migration, but no differences were seen between those derived from normoxic and hypoxic culture conditions. The EV, mainly those derived from hypoxia, increased both mineralization, and the expression of osteoblastic genes. However, they did not affect adipogenesis significantly.

Conclusions: the EV derived from MSC in hypoxia do not affect adipogenesis but have a greater ability to induce osteoblastogenesis. Therefore, they could potentially be used in bone regeneration therapies and treatments for bone conditions like osteoporosis.

Keywords: Extracellular vesicles. Mesenchymal stem cells. Hypoxia. Cell differentiation. Osteoblasts. Adipocytes.

Received: 17/08/2022 • Accepted: 18/04/2023

Authors' contributions: María Ángeles Gálvez-Moreno, and Antonio Casado-Díaz contributed equally to the study.

Conflicts of interest: the authors declare no conflict of interest.

Acknowledgements: Beca FEIOMM de Investigación Traslacional 2016, Proyecto PI18/01659 del Instituto de Salud Carlos III (ISCIII).

Jiménez-Navarro C, Torrecillas-Baena B, Camacho-Cardenosa M, Quesada-Gómez JM, Gálvez-Moreno MA, Casado-Díaz A. Effect of extracellular vesicles derived from hypoxia-preconditioned human mesenchymal stem cells on osteoblastogenesis and adipogenesis *in vitro.* Rev Osteoporos Metab Miner 2023;15(2):54-65

DOI: 10.20960/RevOsteoporosMetabMiner.00012

Correspondence:
Antonio Casado-Díaz. Instituto Maimónides de Investigación Biomédica de Córdoba (IMIBIC). Hospital Universitario Reina Sofía. Avda. Menéndez Pidal, s/n. 14004 Córdoba, Spain
e-mail: bb1cadia@uco.es

INTRODUCTION

Mesenchymal stem cells or MSC (mesenchymal stem cells or mesenchymal stromal cells) are multipotent cells (1,2). The ability of MSC to differentiate into various cell lineages, as well as their anti-inflammatory and immunosuppressive activities has turned them a tool with great potential in cellular therapy and regenerative medicine. MSC participate in the body's homeostasis through tissue regeneration and repair. Osteoblasts are among the cell types MSC can differentiate into. Osteoblastic differentiation is controlled by several signaling pathways including the canonical Wnt/β-catenin pathway, and the increased expression and activation of the transcription factor RUNX2 (3,4). MSC can also differentiate into adipocytes through the induction of the transcription factor PPARγ (peroxisome proliferator-activated receptor γ). This factor regulates the expression of adipogenic genes and induces the development of the adipocytic phenotype (4).

During the aging process or in certain diseases such as diabetes, MSC tend to differentiate into adipocytes at the expense of osteoblastogenesis (5,6). This increases the adiposity of bone marrow, thus decreasing the capacity for bone formation. This favors the loss of bone mass and the onset of osteoporosis (7,8). Therefore, therapeutic strategies that promote osteoblastic differentiation and inhibit adipogenesis can contribute to bone regeneration (9).

The therapeutic applications of MSC face several obstacles. These include the low viability of transplanted cells, their inherent heterogeneity, unidentified factors associated with the age of the donor, and the tumorigenic potential of these cells (10). Recent studies indicate that a large part of the therapeutic properties of MSC are associated with their paracrine effects exerted through their secretome (11) that includes a soluble fraction rich in growth factors and cytokines plus a vesicular fraction that contains various types of molecules with high regenerative capabilities (12). Different studies have shown that there is a synergistic effect when both fractions are used together for regenerative or immunomodulatory purposes (13,14). However, former studies have demonstrated that the vesicular fraction is mainly responsible for the induction of certain potentially regenerative physiological processes. For example, extracellular vesicles (EV) from bone marrow MSC increased the migration and proliferation of dermal fibroblasts in vitro and angiogenesis in human umbilical vein endothelial cells (HUVEC) while EV-depleted conditioned media did not have that effect (15). Due to the regenerative properties of these vesicles and their stability in the medium, the use of MSC-derived EV, instead of the cells themselves, has been proposed as a suitable therapeutic alternative (1,16).

Due to the lack of consensus on the classification of EV, the International Society for Extracellular Vesicles (ISEV) declared that the preferred generic term that should be used is extracellular vesicle (17). The content of EV depends on the type of the original cell and its physiological state. The main components of EV are proteins, lipids, and nucleic acids (RNA and DNA). Proteins, from the family of tetraspanins, stand out among them. CD63, CD81, and CD9 are among the tetraspanins we can find, which are considered exosomal markers (10,18). MicroRNAs (miRNAs) are notable nucleic acids present in EV with the ability to alter gene expression in recipient cells (19). EV participate in intercellular communication, cellular maintenance, immune response, and tumor progression (20). In the case of EV derived from MSC, they play important roles in biological processes like angiogenesis, antigen presentation, apoptosis, coagulation, cellular homeostasis, inflammation, differentiation, proliferation, and intercellular signaling (16).

The use of MSC-derived EV allows us to design cell-free therapies. This can help avoid the difficulties and potential adverse effects associated with the application of cells in cellular therapy (10). Therefore, MSC-derived EV have been evaluated for the treatment of various respiratory, musculoskeletal, cardiovascular, neurological, hepatic, gastrointestinal, dermatological, and renal diseases (21).

The secretion and content of EV vary substantially depending on the physiological state of the MSC from which they derive, which is, in turn, impacted by the environmental conditions of their niche (22). In this context, it has been proven that preconditioning MSC under different culture conditions can stimulate the secretion of EV, thus enhancing their therapeutic efficacy. These conditions include cytokines, hypoxia, trophic and physical factors, as well as chemical and pharmacological agents (23).

The reduced oxygen availability following hypoxia induces a cellular adaptive response that includes alterations in the content of secreted EV (24). At cellular level, hypoxia induces the activation of hypoxia-inducible factor 1-alpha (HIF1α). Under normoxic conditions, this transcription factor is hydroxylated and degraded by the cytoplasmic proteasome. However, in the presence of tissue damage, ischemic processes, or exposure to hypoxia, the decreased availability of oxygen inhibits the hydroxylation of HIF1α, thus leading to its accumulation and translocation into the nucleus where it induces the expression of genes involved in the adaptation of low oxygen levels. These genes include those associated with angiogenesis, wound healing, anaerobic glucose metabolism, erythropoiesis, proliferation, differentiation, and apoptosis, among others. It has been demonstrated that hundreds of genes can be transcriptionally regulated by HIF1α (25). Regarding the effect of hypoxia on the content of EV, numerous studies have shown that MSC-derived EV preconditioned under hypoxia have greater therapeutic capabilities in regenerative medicine (24).

Although it is known that the paracrine effects of MSC mediated by secretion affect various cellular physiological aspects, there is still limited information on how these vesicles can influence the adipogenic and osteogenic differentiation of precursor cells. Therefore, the objective of this study was to investigate how EV derived from cultures of human bone marrow MSC grown under hypoxic or normoxic conditions affect the osteoblastic and adipogenic differentiation of MSC. The aim is to contribute to the necessary knowledge for the possible development of new therapeutic approaches for the management of conditions associated with bone and/or adipose tissue.

MATERIALS AND METHODS

CULTURE AND EXPANSION OF MESENCHYMAL STEM CELLS

Human bone marrow derived MSC were obtained from cryopreserved and previously characterized cultures from our group's cell line collection. MSC from a healthy 31-year-old male donor were used for this study. A vial of cryopreserved MSC (8×10^5 cells) was seeded into a 75 cm^2 culture flask in a α-MEM culture medium (Cambrex Bio Science-Lonza; Basel, Switzerland) supplemented with 10 % FBS (Gibco-Thermo Fisher Scientific), 1 % ultraglutamine (Cambrex Bio Science-Lonza), 0.1 mg/mL streptomycin, 100 U of penicillin, and 1 ng/mL FGF-2 (Fibroblast Growth Factor-2) from Sigma-Aldrich (Saint Louis, MO, United States). The culture medium was changed every 3-4 days. Upon reaching 80 %-90 % confluency, the cells were detached using trypsin-EDTA (Gibco-Thermo Fisher Scientific) and re-seeded in 1:3 dilution.

ISOLATION OF MSC-DERIVED EXTRACELLULAR VESICLES

In MSC cultures at passages 4 to 6, when they reached approximately 70 % confluency, the culture medium was replaced with a fresh medium supplemented with 5 % exosome-depleted FBS (Gibco-Thermo Fisher Scientific). Cells were maintained in this medium for 48 hours under 2 oxygen concentration conditions: hypoxia (5 % CO_2, 3 % O_2, and 37 °C) and normoxia (5 % CO_2, 16 % O_2, and 37 °C). Afterwards, the culture medium from three 75 cm^2 flasks (approximately 50 mL) for each condition was collected and centrifuged at 4 °C for 10 min at 300 g, 20 min at 1200 g, and 30 min at 10 000 g. After the final centrifugation, the culture medium was concentrated using the Amicon®Ultra-15 Centrifugal Filter Device 100 kDa (Millipore; Merck KGaA, Darmstadt, Germany) to approximately 2 mL. EV were purified from the concentrated medium using size-exclusion chromatography with PURE-EV Columns (HansaBioMed; Tallinn, Estonia) following the manufacturer's instructions for use. The EV-containing fractions were finally concentrated to a volume of 300-400 µL using ultrafiltration with an Amicon®Ultra-15 Centrifugal Filter Device 10 kDa (Millipore).

MORPHOLOGICAL CHARACTERIZATION AND QUANTIFICATION OF EXTRACELLULAR VESICLES

The morphology of EV was analyzed using transmission electron microscopy (TEM). In short, 20 µL of the sample were applied to carbon-coated copper grids. After drying, the grids were stained with 2 % (w/v) uranyl acetate (UrAc) for 1 min. Images were captured using a JEOL JEM 1400 High-resolution transmission electron microscope (SCAI, University of Córdoba, Córdoba, Spain) at an acceleration voltage of 80-200 keV.

The nanoparticle concentration was determined using a Nanosight NS300 at the University Institute of Nanochemistry, Universidad de Córdoba, Córdoba, Spain.

Western blotting

For total protein extraction from different cell cultures, cells were lysed with the Cell Extraction Buffer (Thermo Fisher Scientific) that was supplemented with 1 mM phenylmethylsulfonyl fluoride (PMSF) and a 50 µL/mL protease inhibitor cocktail (PIC) (both from Sigma-Aldrich). The lysate was incubated on ice for 30 min with vortexing every 10 min. Finally, the lysate was centrifuged for 10 min at 13 000g at 4 °C, the precipitated cellular debris was discarded, and the supernatant was stored at -20 °C until further use. Protein concentration was quantified using the Bio-Rad DC Protein Assay kit (Bio-Rad) following the manufacturer's protocol. For the extraction and quantification of proteins from EV, the same protocol was used after lysing the vesicles with the Cell Extraction Buffer.

The protein concentration obtained from EV ranged from 0.1 µg/µL to 0.3 µg/µL. For Western blotting, a total of 2 µg to 10 µg of protein from each sample were loaded onto an 8 %-16 % acrylamide gel (nUView Tris-Glycine Precast Gels, NuSeP) in denaturing conditions using a Mini-Protean electrophoresis system (Bio-Rad). After electrophoresis, proteins were transferred to Polyvinylidene difluoride (PVDF) membranes (Bio-Rad) using a Trans-Blot Turbo Transfer System (Bio-Rad). The membranes were blocked with a 5 % non-fat dry milk solution in T-TBS buffer (20 mM Tris-HCl pH 7.6, 150 mM NaCl, 0.05 % Tween) for 1 hour at room temperature. Afterwards, the membranes were

incubated overnight at 4 °C with primary antibodies, anti-CD9 (1:700), anti-CD63 (1:700) (both from Invitrogen, ThermoFisher Scientific), or anti-calnexin (1:1000) from Sigma-Aldrich, in 1 % milk in T-TBS. After washing the membranes 3 times with T-TBS, they were incubated with the secondary antibody, anti-Mouse IgG H & L-HRP (1:5000) (Invitrogen, ThermoFisher Scientific) for CD9 and CD63, and anti-Rabbit IgG H & L-HRP (1:3000) (Abcam) for calnexin, in 1 % milk in T-TBS for 1 hour. Finally, the excess secondary antibody was washed with T-TBS, and the membrane was developed using Clarity Western ECL Substrate (Bio-Rad). The bands were visualized using a Bio-Rad ChemiDoc™ XRS+ Gel Documentation System through the ImageLab software from the same company. The band intensity was later quantified using ImageJ 1.53t software.

QUANTIFICATION OF GENE EXPRESSION THROUGH POLYMERASE CHAIN REACTION (PCR)

RNA from cultures induced to differentiate into osteoblasts or adipocytes was isolated using the NZY total RNA isolation kit (NZYTech Lda; Lisbon, Portugal) following the manufacturer's instructions for use. RNA was quantified using a NanoDrop ND-1000 spectrophotometer from Thermo Fisher Scientific, and 900 ng were reverse transcribed into cDNA using the iScript cDNA Synthesis Kit (Bio-Rad) again according to the manufacturer's instructions for use.

Real-time quantitative PCR (qRT-PCR) was performed using a Roche Applied Science LightCycler 96 Instrument. Each PCR reaction was performed in a volume of 10 µL containing 1 µL of cDNA, 1 µM primers (Table I), and 1X SensiFAST Sybr No-Rox Mix (BIOLINE). The PCR amplification program included an initial cycle at 95 °C for 2 min (DNA denaturation and activation of DNA polymerase) and 40 to 45 cycles of 95 °C for 5 seconds (DNA denaturation) at 65 °C for 30 seconds (primer annealing and product extension). The results were analyzed using the LightCycler 1.1 software from the same manufacturer. The POLR2A gene (polymerase [RNA; DNA-directed] II polypeptide A) was used as a constitutive gene.

CELL VIABILITY ASSAY

Cell viability was determined using 3-(4,5-dimethylthiazol-2-yl)-2,5-diphenyltetrazolium bromide (MTT) (Sigma-Aldrich). MSC were seeded in 96-well plates at a density of 4000 cells per well in culture medium. Cells were treated in a culture medium supplemented with EV-free FBS and different concentrations of MSC-derived EV kept under normoxic culture conditions (MSC-EvN) or hypoxia (MSC-EvH) (3×10^7, 9×10^7, and 15×10^7 particles/mL). After 48 hours, the culture medium was removed, and 100 µL of DMEM (Dulbecco's Modified Eagle Medium; Capricorn Scientific GmbH) without FBS or phenol red, containing 1 mg/mL MTT, were added. Cells were incubated at 37 °C for 2 hours,

Table I. Primer sequences and amplicon sizes

Gene	Direct and reverse primer sequence (5 '→ 3')	Size of byproduct (bp)
Runt-related transcription factor 2 *(RUNX2)*	TGGTTAATCTCCGCAGGTCAC ACTGTGCTGAAGAGGCTGTTTG	143
Osterix *(SP7)*	AGCCAGAAGCTGTGAAACCTC AGCTGCAAGCTCTCCATAACC	163
Collagen, type I, alpha 1 *(COL1A1)*	CGCTGGCCCCAAAGGATCTCCTG GGGGTCCGGGAACACCTCGCTC	263
Integrin-binding sialoprotein *(BSP)*	AGGGCAGTAGTGACTCATCCG CGTCCTCTCCATAGCCCAGTGTTG	171
Peroxisome proliferator-activated receptor gamma 2 *(PPARG2)*	GCGATTCCTTCACTGATACACTG GAGTGGGAGTGGTCTTCCATTAC	136
Lipoprotein lipase *(LPL)*	AAGAAGCAGCAAAATGTACCTGAAG CCTGATTGGTATGGGTTTCACTC	113
Fatty-acid-binding protein 4 *(FABP4)*	TCAGTGTGAATGGGGATGTGAT TCTGCACATGTACCAGGACACC	162
Fatty acid synthase *(FASN)*	AAGCTGAAGGACCTGTCTAGG CGGAGTGAATCTGGGTTGATG	146
Polymerase (RNA; DNA directed) II polypeptide A *(POLR2A)*	TTTTGGTGACGACTTGAACTGC CCATCTTGTCCACCACCTCTTC	125

and the formazan crystals formed during incubation were dissolved in 100 % isopropanol. The absorbance of the resulting solution was measured at 570 nm, with a reference at 650 nm using a PowerWave XS microplate spectrophotometer (BioTek Instruments).

CELL MIGRATION ASSAY

Cell migration of MSC was evaluated using the Oris™ Cell Migration Assay (Platypus Technologies). MSC were seeded in 96-well plates (15 000 cells/well) and incubated at 37°C with cell seeding stoppers in each well until reaching 90 % confluency. Afterwards, the stoppers were removed, leaving a 2 mm halo in the center of each well. After washing with PBS, α-MEM + 2 % EV-free FBS was added containing MSC-EvN or MSC-EvH at a concentration of 3×10^7, 9×10^7, or 15×10^7 particles/mL. At 0 h, 12 h, and 18 h, images were captured using an Incucyte® Systems for Live-Cell Imaging phase-contrast microscope. Migration was measured by calculating the percentage of wound closure area compared to the initial open area (t = 0) using the following formula: migration area (%) = (A0-At)/A0 × 100, where A0 represents the initial open area, and At the residual area at the measurement time. ImageJ software was used to quantify areas in the images.

ADIPOCYTE AND OSTEOBLAST DIFFERENTIATION

MSC were seeded in P12 or P24 culture plates (Nalgene-Nunc-Thermo Fisher Scientific) at a density of 3000 cells/cm^2. Once they reached 60 %-80 % confluency, they were differentiated into adipocytes or osteoblasts in the presence or absence of MSC-EvN or MSC-EvH. To induce adipocyte differentiation, the culture medium without FGF was supplemented with 5×10^{-7}M dexamethasone, 50 µM indomethacin, and 0.5 mM isobutylmethylxanthine. For osteoblast differentiation, the medium was supplemented with 10^{-8} M dexamethasone, 10 mM β-glycerophosphate, and 0.2 mM ascorbic acid. All inducers were obtained from Sigma-Aldrich.

After 13 days of differentiation, samples were taken from the cultures for RNA extraction and analysis of gene expression of adipocyte or osteoblast markers.

MINERALIZATION STAINING OF THE EXTRACELLULAR MATRIX

Mineralization of the matrix in osteoblast-induced MSC was evaluated using alizarin red S staining at 21 days. Cultures were fixed for 10 min with 3.7 % formaldehyde and stained with a 40 mM alizarin red S solution at pH 4.1. All reagents were from Sigma-Aldrich. The wells were then washed with 60 % isopropanol, dried, and images were captured. To quantify mineralization, the staining was eluted with 10 % acetic acid and neutralized with 10 % ammonium hydroxide. The resulting solution's absorbance was measured at 405 nm using a PowerWave XS microplate spectrophotometer from BioTek Instruments.

OIL RED STAINING OF LIPID DROPLETS

The formation of lipid droplets in adipocyte-induced cultures was evaluated using oil-red O staining at 13 days of differentiation. Cultures were fixed with 3.7 % formaldehyde for 20 min and stained with a solution of 60 % 0.3 % oil-red (w/v in isopropanol) and 40 % distilled water. After 15 to 20 min of incubation, cells were washed with distilled water, stained with hematoxylin, and images were taken using an optical microscope for each well. Oil-red O staining was quantified using image analysis software ImageJ. The area of the oil-red O stained image was normalized to the corresponding cell number.

STATISTICAL ANALYSIS

Comparison between different treatments was performed using ANOVA to detect significant changes followed by Tukey's test to identify significant differences between pairs of treatments. Significant changes (*) were considered with p values < 0.05. At least 3 data points were obtained per studied parameter. Data are expressed as mean ± standard error of the mean (mean ± SEM).

RESULTS

CHARACTERIZATION OF EXTRACELLULAR VESICLES

In size exclusion chromatography of concentrated media from MSC grown under normoxic or hypoxic culture conditions, 10 fractions were obtained and their protein concentration was estimated by measuring absorbance at 280 nm. As shown on figure 1A, the amount of eluted protein increased from fraction

7 onwards, which is indicative that protein-free EV are present in previous fractions.

After mixing and subsequent concentration of fractions 1 to 6 by ultrafiltration, the nanovesicles obtained were quantified and analyzed by Nanoparticle Tracking Analysis. The average size of the EV obtained from this analysis was approximately 150 nm (Fig. 1B). Transmission electron microscopy (TEM) images showed the spherical morphology of the isolated EVs (Fig. 1C). Furthermore, the presence of surface markers CD63 and CD9 were detected in the nanovesicles while the cellular protein calnexin was not detected (Fig. 1D).

EFFECT OF MSC-EvN AND MSC-EvH APPLICATION ON MSC VIABILITY AND MIGRATION

MSC were grown in the presence or absence of 30, 60, or 150 x 10^6 particles/mL of MSC-EvN or MSC-EvH for 3 days, time after which cell viability was quantified. As shown in figure 2A, MSC viability tended to increase with the concentration of EV. This increase was significant with the highest concentration used for both types of EV being slightly higher in cells treated with EV derived from hypoxia conditions (Fig. 2A).

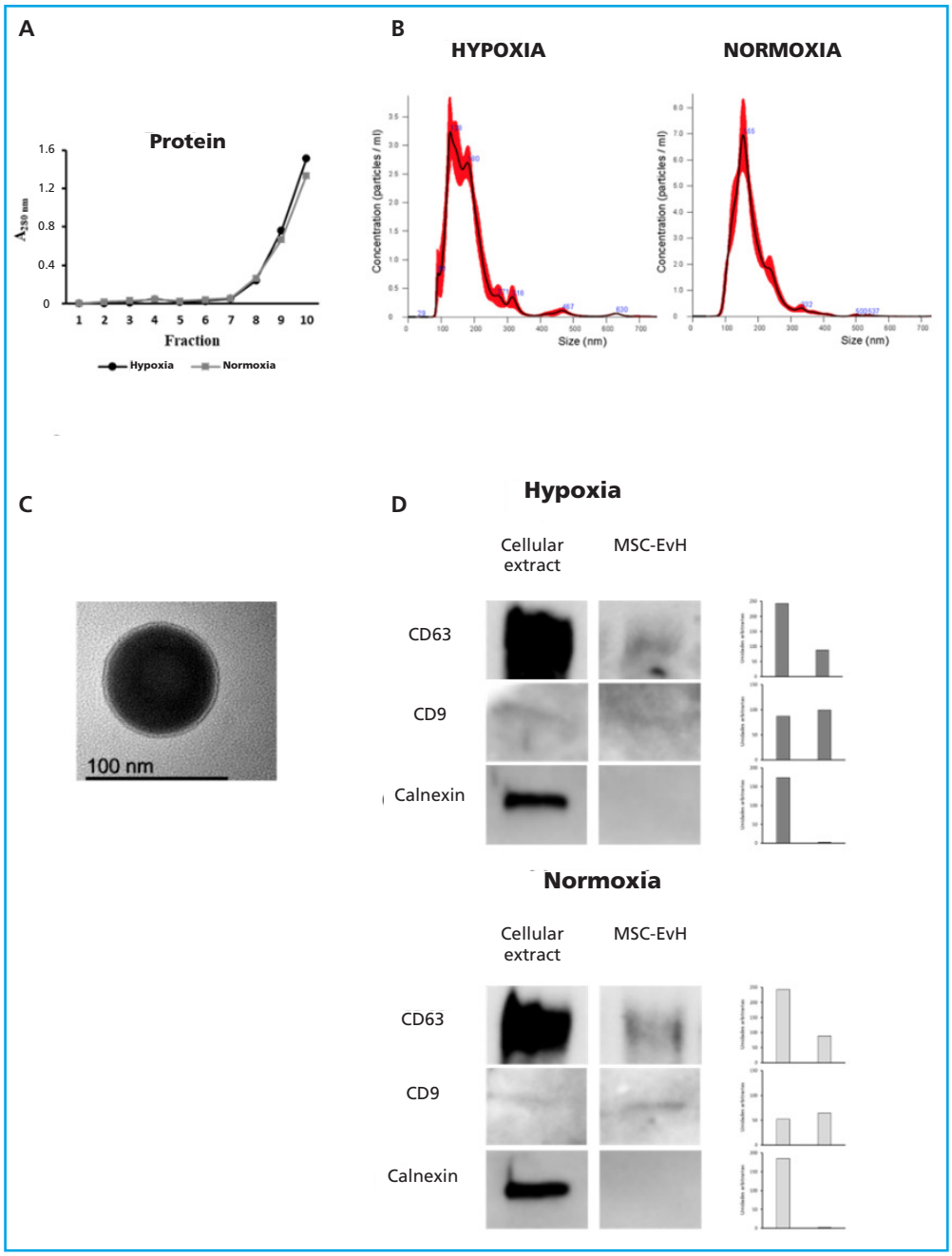

Figure 1. Characterization of extracellular vesicles derived from MSC in normoxic and hypoxic conditions. A. Absorbance at 280 nm of the fractions obtained through size exclusion chromatography. B. Particle size distribution of MSC-EvN and MSC-EvH obtained through Nanosight. C. TEM image of an EV showing its morphology and size. D. Western blot analysis of the protein expression pf positive EV markers (CD63 and CD9) and negative markers (calnexin) in cell and EV extracts (MSC-EvH and MSC-EvN). The graphical representation of their expression quantification is shown to the left of each marker.

Cell migration of MSC in the presence of different EV concentrations also tended to be higher. However, these changes were not significant in the case of treatments with MSC-EvH. On the other hand, MSC-EvN treatment increased cell migration significantly, but only when the highest concentration was used (Fig. 2B).

EFFECT OF EXTRACELLULAR VESICLES ON MSC DIFFERENTIATION INTO OSTEOBLASTS

Considering the results obtained regarding MSC viability and migration, a concentration of 15 × 10^7 particles/mL of MSC-EvN and MSC-EvH was selected to study and assess their effect on cell differentiation.

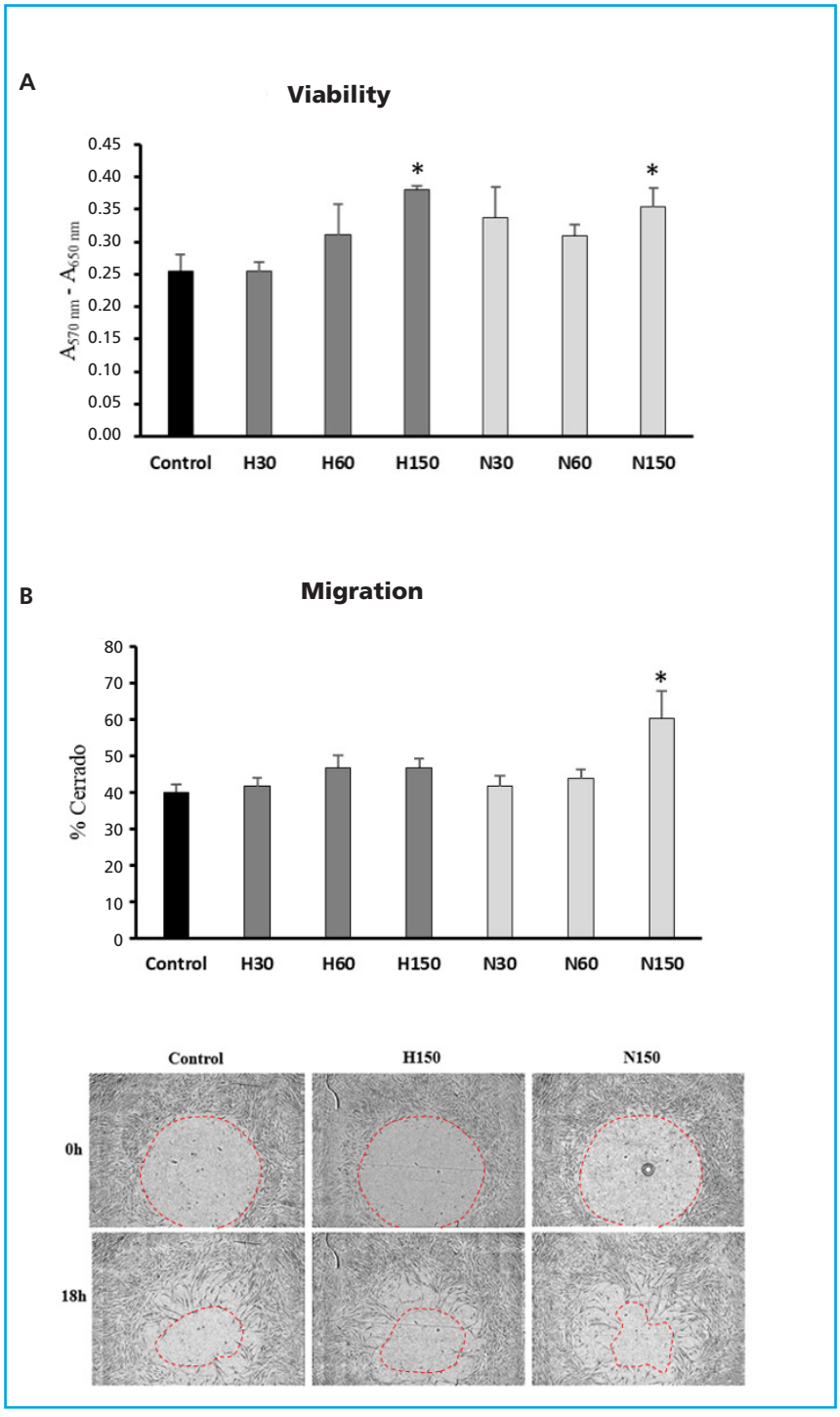

Figure 2. Viability and migration of MSC in the presence or absence of MSC-EvH or MSC-EvN. A. Effect of treatment with MSC-EvH (H) or MSC-EvN (N) at concentrations of 3 × 10^7 particles/mL (30), 6 × 10^7 particles/mL (60), and 15 × 10^7 particles/mL (150) on MSC culture viability. B. Same as (A), but for cell migration. The images represent representative cultures treated 0 and 18 h after the start of migration. *$p < 0.05$ vs control (untreated cells).

Mineralization of MSC differentiated into osteoblasts increased significantly with both types of vesicles. This increase was higher in cultures treated with EV derived from cultures under hypoxia conditions (Fig. 3A). Regarding the expression of osteoblastic marker genes, no significant changes were found in the genes encoding the transcription factor RUNX2 and the extracellular matrix protein collagen type 1 alpha (COL1A1). However, a significant increase was observed in the expression of the SP7 transcription factor gene, also known as osterix, with MSC-EvH treatment. Additionally, treatments with MSC-EvH and MSC-EvN significantly induced the expression of the integrin-binding sialoprotein gene (IBSP). In this case, the change was greater in EV derived from MSC in hypoxia compared to those obtained from normoxic culture conditions (Fig. 3B). These results suggest that EV derived from MSC in hypoxia have a greater capacity to promote osteoblastogenesis compared to those obtained from cultures obtained in normoxic conditions.

EFFECT OF EXTRACELLULAR VESICLES ON MSC DIFFERENTIATION INTO ADIPOCYTES

In the phenotypic analysis of MSC differentiated into adipocytes treated with MSC-EvH or MSC-EvN, no significant changes were seen in the formation of fat vesicles

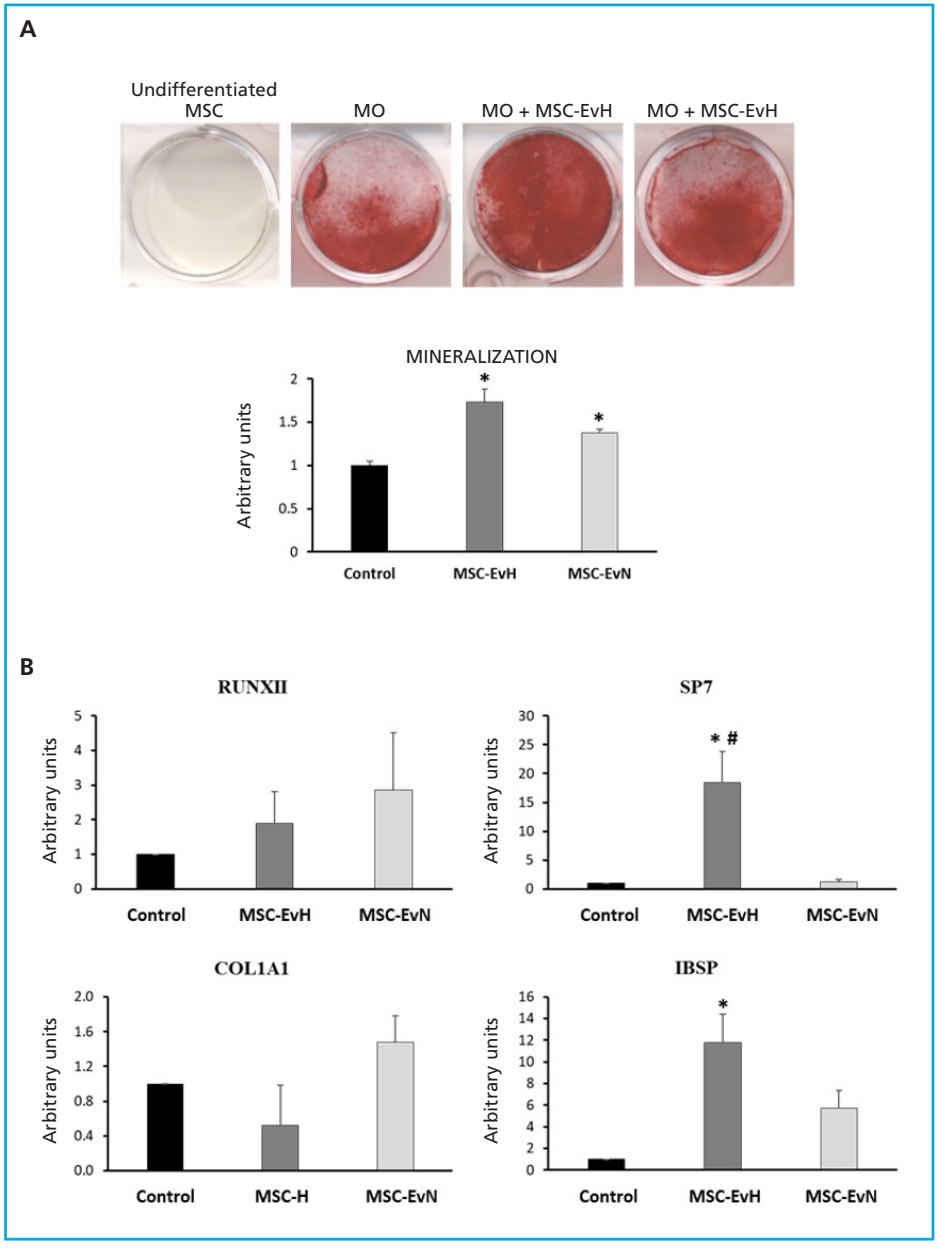

Figure 3. Effect of extracellular vesicles derived from MSC on osteogenic differentiation. A. Representative images and quantification of alizarin red S staining of MSC cultures at 21 days of differentiation in osteoblastic medium (OM) in the presence or absence of MSC-EvH or MSC-EvN. B. Expression of osteogenic genes RUNX2, SP7, COL1A1, and IBSP at 13 days of differentiation in cultures treated with MSC-EvH and MSC-EvN. Data are expressed as mean ± SEM. *$p < 0.05$ vs control (untreated cultures); #$p < 0.05$ vs MSC-EvN.

compared to untreated cultures (Fig. 4A). Regarding the expression of adipogenic genes PPARG2, LPL, and FASN, no differences were seen between the different treatments and the control. However, the expression of FABP4 in cultures treated with MSC-EvN increased significantly compared to the control and cultures treated with MSC-EvH. The expression of the latter showed no changes compared to untreated cultures (Fig. 4B).

DISCUSSION

Our study demonstrates that size exclusion chromatography for EV isolation produces highly pure vesicles with low contamination of soluble proteins (26). The results of treatments with both types of EV, MSC-EvH and MSC-EvN, indicate that they increase the viability

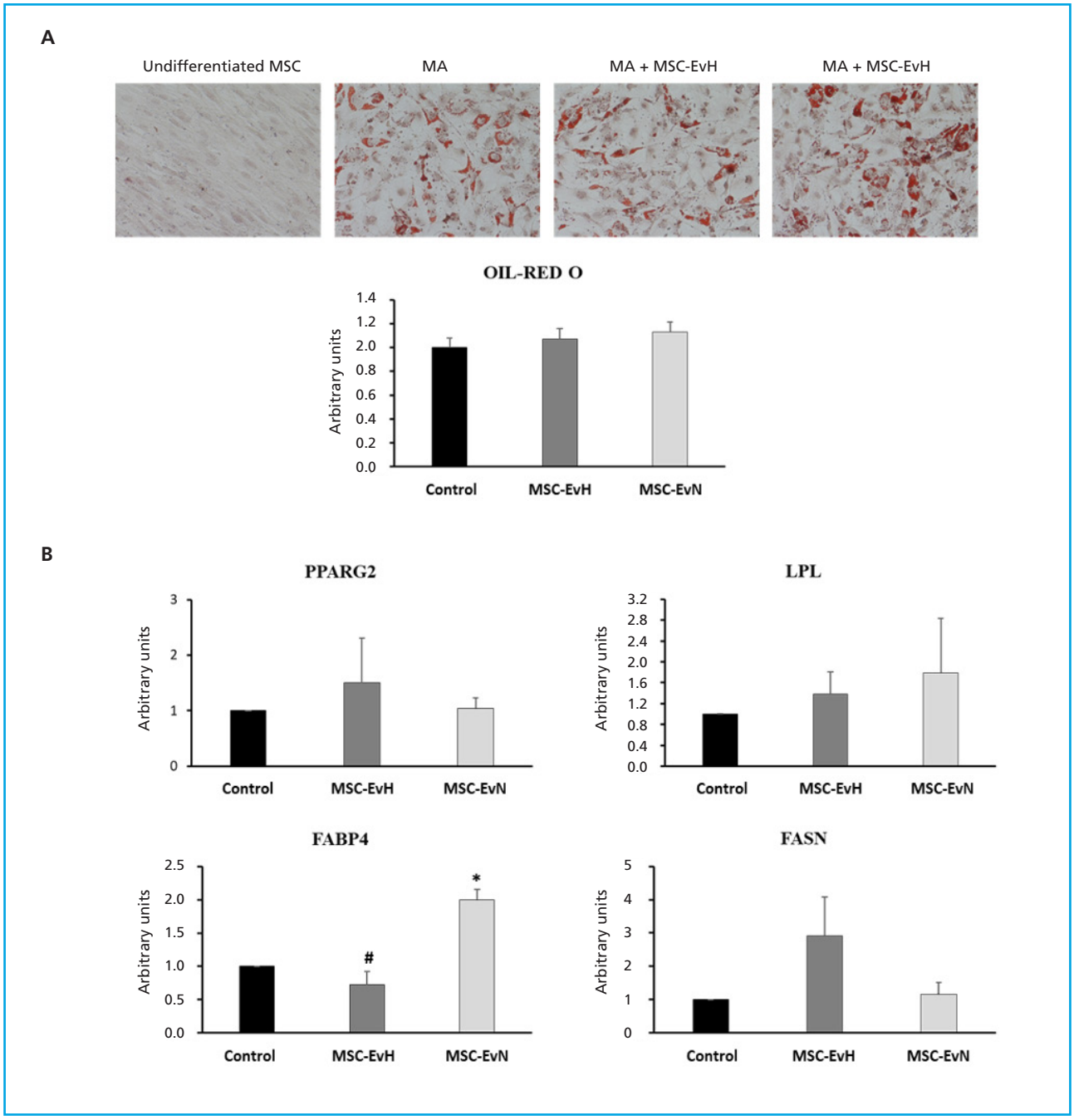

Figure 4. Effect of extracellular vesicles derived from MSC on adipogenic differentiation. A. Images and quantification of oil red O staining in MSC cultures after 13 days in adipogenic medium (AM) in the presence or absence of MSC-EvH or MSC-EvN. (Images at 200x magnification). B. Expression of adipogenic genes PPARG2, LPL, FABP4, and FASN at 13 days of differentiation in cultures treated with MSC-EvH and MSC-EvN. Data are expressed as mean ± SEM. *$p < 0.05$ vs control (untreated cultures); #$p < 0.05$ vs MSC-EvN.

of MSC cultures in vitro when applied at a concentration of 15 × 10^7 particles/mL. The positive effect of EV derived from MSC on the viability of different cell types has been described in various studies (15,27). Some authors have shown that MSC-derived EV do not affect the viability of bone marrow-derived MSC (28). However, these results were obtained from EV obtained by ultracentrifugation and after maintaining the cells for 12 hours in fresh culture media (28), not 48 hours as it was our case. Therefore, the different methodological conditions can affect the content of EV and explain the differences seen among different studies. Our data do not show differences between the effects of MSC-EvH and MSC-EvN on the viability of MSC cultures. However, some authors have described that EV derived from MSC cultured in hypoxic conditions have a greater capacity to increase cell viability compared to those obtained in normoxic conditions (29,30). However, we should mention that these studies have been mainly conducted on endothelial cells, not MSC. We should, therefore, remember that hypoxia causes the production of factors that stimulate and induce endothelial cells to form new vessels to compensate for the decreased oxygen levels like the vascular endothelial growth factor (VEGF) (31). These factors may be abundant in EV derived from MSC maintained in hypoxic conditions. However, our data suggest that they may not have a significant effect on the viability MSC.

Treatment with MSC-EvH and MSC-EvN tended to increase MSC migration. In other cell types such as endothelial cells, fibroblasts, and keratinocytes, it has been shown that MSC-derived EV enhance their proliferation and migration capabilities (32,33). The increased migration induction is associated with greater regenerative capabilities of EV (34). Our results show that MSC migration was not significantly influenced when treated with MSC-EvH. This suggests that the hypoxic culture conditions used did not produce EV enriched in factors that would stimulate the migration of these cells.

The use of EV derived from bone cells like bone marrow MSC is emerging as a possible therapeutic strategy to treat bone conditions including osteoporosis (35,36). Our results show that in vitro osteogenic differentiation of MSC is enhanced when cultures are treated with EV derived from MSC, primarily with MSC-EvH. Cultures treated with these EV exhibited greater mineralization and expression of osteoblastic genes such as *SP7* and *IBSP*. The former encodes a transcription factor essential for osteogenic differentiation (37) while the latter encodes integrin-binding sialoprotein, an extracellular matrix protein involved in mineralization (38). These results support what has been previously described by other studies demonstrating the osteogenic capabilities of EV obtained from MSC (39-41). *In vivo* experiments in a bone fracture model have shown that EV derived from MSC cultured under hypoxic conditions promote bone fracture healing to a greater extent compared to EV obtained from MSC under normoxic conditions. This is partly due to their promotion of angiogenesis through miR-126, which regulates the SPRED1/Ras/Erk angiogenic signaling pathway (40). In our case, we have not evaluated the potential effect of MSC-EvH on endothelial cells, but we have demonstrated that they induce osteoblastogenesis in precursor cells. Therefore, treatment with MSC-EvH could promote bone regeneration through its induction of angiogenesis in endothelial cells and osteoblastic differentiation of MSC. Other studies also support the high potential of MSC-derived EV regarding bone regeneration due to their ability to promote angiogenesis and osteoblastogenesis (39). The positive effect of MSC-derived EV on osteoblastogenesis *in vitro* and *in vivo* has been observed to involve miRNAs such as miR-196a, miR-335, and miR-27a (41-43).

MSC are also precursors of adipocytes. Overall, factors that promote adipogenic differentiation negatively affect osteogenesis and vice versa (9). However, our results indicate that neither MSC-EvH nor MSC-EvN affected adipogenesis significantly. Only the mRNA levels of FABP4 increased with MSC-EvN treatment. The FABP4 gene encodes a fatty acid-binding protein involved in various extracellular functions, so the application of MSC-EvN may affect aspects related to fatty acid metabolism during adipogenesis (44), which in our case did not affect the accumulation of lipid droplets.

In conclusion, our data demonstrate that treatment with MSC-derived EV enhances the viability, migration, and osteogenic differentiation of human bone marrow MSC. Osteoblastic differentiation is primarily induced when EV are derived from MSC exposed to hypoxia. This suggests that preconditioning cells under low oxygen levels could induce the secretion of EV enriched in osteogenic factors. The identification of these factors in the future may provide insights into the mechanism of action of these EV regarding osteoblastogenesis opening up other possibilities to design more efficient therapeutic strategies to treat different bone conditions. The results of this study support the potential use of cell-free therapy based on the application of EV to treat systemic bone diseases like osteoporosis and promote bone formation in difficult-to-heal fractures.

REFERENCES

1. Kim S, Lee SK, Kim H, et al. Exosomes secreted from induced pluripotent stem cell-derived mesenchymal stem cells accelerate skin cell proliferation. Int J Mol Sci 2018;19:3119. DOI: 10.3390/ijms19103119
2. Rani S, Ryan AE, Griffin MD, et al. Mesenchymal stem cell-derived extracellular vesicles: Toward cell-free therapeutic applications. Mol Ther 2015;23:812-23. DOI: 10.1038/mt.2015.44
3. Gomathi K, Akshaya N, Srinaath N, et al. Regulation of Runx2 by post-translational modifications in osteoblast differentiation. Life Sci 2020;245:117389. DOI: 10.1016/j.lfs.2020.117389

4. Takada I, Kouzmenko AP, Kato S. Wnt and PPARγ signaling in osteoblastogenesis and adipogenesis. Nat Rev Rheumatol 2009;5:442-7. DOI: 10.1038/nrrheum.2009.137
5. Moerman EJ, Teng K, Lipschitz DA, et al. Aging activates adipogenic and suppresses osteogenic programs in mesenchymal marrow stroma/stem cells: The role of PPAR-γ2 transcription factor and TGF-β/BMP signaling pathways. Aging Cell 2004;3:379-89. DOI: 10.1111/j.1474-9728.2004.00127.x
6. Singh L, Brennan T, Russell E, et al. Aging alters bone-fat reciprocity by shifting in vivo mesenchymal precursor cell fate towards an adipogenic lineage. Bone 2016;85:29-36. DOI: 10.1016/j.bone.2016.01.014
7. Qadir A, Liang S, Wu Z, et al. Senile osteoporosis: The involvement of differentiation and senescence of bone marrow stromal cells. Int J Mol Sci 2020;21:349. DOI: 10.3390/ijms21010349
8. Rosen CJ, Bouxsein ML. Mechanisms of disease: is osteoporosis the obesity of bone? Nat Clin Pract Rheumatol 2006;2:35-43. DOI: 10.1038/ncprheum0070
9. Chen Q, Shou P, Zheng C, et al. Fate decision of mesenchymal stem cells: adipocytes or osteoblasts? Cell Death Differ 2016;23:1128-39. DOI: 10.1038/cdd.2015.168
10. Joo HS, Suh JH, Lee HJ, et al. Current knowledge and future perspectives on mesenchymal stem cell-derived exosomes as a new therapeutic agent. Int J Mol Sci 2020;21:727. DOI: 10.3390/ijms21030727
11. Kusuma GD, Carthew J, Lim R, et al. Effect of the Microenvironment on Mesenchymal Stem Cell Paracrine Signaling: Opportunities to Engineer the Therapeutic Effect. Stem Cells Dev 2017;26:617-31. DOI: 10.1089/scd.2016.0349
12. Vizoso FJ, Eiro N, Cid S, et al. Mesenchymal stem cell secretome: Toward cell-free therapeutic strategies in regenerative medicine. Int J Mol Sci 2017;18(9):1852. DOI: 10.3390/ijms18091852
13. Vilaça-Faria H, Marote A, Lages I, et al. Fractionating stem cells secretome for Parkinson's disease modeling: Is it the whole better than the sum of its parts? Biochimie 2021;189:87-98. DOI: 10.1016/j.biochi.2021.06.008
14. González-Cubero E, González-Fernández ML, Olivera ER, et al. Extracellular vesicle and soluble fractions of adipose tissue-derived mesenchymal stem cells secretome induce inflammatory cytokines modulation in an in vitro model of discogenic pain. Spine J 2022;22:1222-34. DOI: 10.1016/j.spinee.2022.01.012
15. Shabbir A, Cox A, Rodriguez-Menocal L, et al. Mesenchymal Stem Cell Exosomes Induce Proliferation and Migration of Normal and Chronic Wound Fibroblasts, and Enhance Angiogenesis in Vitro. Stem Cells Dev 2015;24:1635-47. DOI: 10.1089/scd.2014.0316
16. Casado-Díaz A, Quesada-Gómez JM, Dorado G. Extracellular Vesicles Derived From Mesenchymal Stem Cells (MSC) in Regenerative Medicine: Applications in Skin Wound Healing. Front Bioeng Biotechnol 2020;8:1-19. DOI: 10.3389/fbioe.2020.00146
17. Théry C, Witwer KW, Aikawa E, et al. Minimal information for studies of extracellular vesicles 2018 (MISEV2018): a position statement of the International Society for Extracellular Vesicles and update of the MISEV2014 guidelines. J Extracell Vesicles 2018;7:1535750. DOI: 10.1080/20013078.2018.1535750
18. Jeppesen DK, Fenix AM, Franklin JL, et al. Reassessment of Exosome Composition. Cell 2019;177:428-45.e18. DOI: 10.1016/j.cell.2019.02.029
19. Deng H, Sun C, Sun Y, et al. Lipid, Protein, and MicroRNA Composition Within Mesenchymal Stem Cell-Derived Exosomes. Cell Reprogram 2018;20:178-86. DOI: 10.1089/cell.2017.0047
20. Doyle L, Wang M. Overview of Extracellular Vesicles, Their Origin, Composition, Purpose, and Methods for Exosome Isolation and Analysis. Cells 2019;8:727. DOI: 10.3390/cells8070727
21. Willis GR, Kourembanas S, Mitsialis SA. Toward Exosome-Based Therapeutics: Isolation, Heterogeneity, and Fit-for-Purpose Potency. Front Cardiovasc Med 2017;4:63. DOI: 10.3389/fcvm.2017.00063
22. Costa LA, Eiro N, Fraile M, et al. Functional heterogeneity of mesenchymal stem cells from natural niches to culture conditions: implications for further clinical uses. Cellular and Molecular Life Sciences 2021;78:447-67. DOI: 10.1007/s00018-020-03600-0
23. Ding J, Wang X, Chen B, et al. Exosomes Derived from Human Bone Marrow Mesenchymal Stem Cells Stimulated by Deferoxamine Accelerate Cutaneous Wound Healing by Promoting Angiogenesis. Biomed Res Int 2019;2019:9742765. DOI: 10.1155/2019/9742765
24. Pulido-Escribano V, Torrecillas-Baena B, Camacho-Cardenosa M, et al. Role of hypoxia preconditioning in therapeutic potential of mesenchymal stem-cell-derived extracellular vesicles. World J Stem Cells 2022;14:453-72. DOI: 10.4252/wjsc.v14.i7.453
25. Mole D, Blancher C, Copley R, et al. Genome-wide association of hypoxia-inducible factor (HIF)-1alpha and HIF-2alpha DNA binding with expression profiling of hypoxia-inducible transcripts. J Biol Chem 2009;284:16767-75. DOI: 10.1074/jbc.M901790200
26. Gámez-Valero A, Monguió-Tortajada M, Carreras-Planella L, et al. Size-Exclusion Chromatography-based isolation minimally alters Extracellular Vesicles' characteristics compared to precipitating agents. Sci Rep 2016;6:1-9. DOI: 10.1038/srep33641
27. Wang Y, Yao J, Cai L, et al. Bone-targeted extracellular vesicles from mesenchymal stem cells for osteoporosis therapy. Int J Nanomedicine 2020;15:7967-77. DOI: 10.2147/IJN.S263756
28. Wei F, Li Z, Crawford R, et al. Immunoregulatory role of exosomes derived from differentiating mesenchymal stromal cells on inflammation and osteogenesis. J Tissue Eng Regen Med 2019;13:1978-91. DOI: 10.1002/term.2947
29. Almeria C, Weiss R, Roy M, et al. Hypoxia Conditioned Mesenchymal Stem Cell-Derived Extracellular Vesicles Induce Increased Vascular Tube Formation in vitro. Front Bioeng Biotechnol 2019;7:1-12. DOI: 10.3389/fbioe.2019.00292
30. Gao W, He R, Ren J, et al. Exosomal HMGB1 derived from hypoxia-conditioned bone marrow mesenchymal stem cells increases angiogenesis via the JNK/HIF-1α pathway. FEBS Open Bio 2021;11:1364-73. DOI: 10.1002/2211-5463.13142
31. Han Y, Ren J, Bai Y, et al. Exosomes from hypoxia-treated human adipose-derived mesenchymal stem cells enhance angiogenesis through VEGF/VEGF-R. Int J Biochem Cell Biol 2019;109:59-68. DOI: 10.1016/j.biocel.2019.01.017
32. Ren S, Chen J, Duscher D, et al. Microvesicles from human adipose stem cells promote wound healing by optimizing cellular functions via AKT and ERK signaling pathways 06 Biological Sciences 0601 Biochemistry and Cell Biology. Stem Cell Res Ther 2019;10:1-14.
33. Wang X, Omar O, Vazirisani F, et al. Mesenchymal stem cell-derived exosomes have altered microRNA profiles and induce osteo-

genic differentiation depending on the stage of differentiation. PLoS One 2018;13:4-6. DOI: 10.1371/journal.pone.0193059
34. Cooper DR, Wang C, Patel R, et al. Human Adipose-Derived Stem Cell Conditioned Media and Exosomes Containing MALAT1 Promote Human Dermal Fibroblast Migration and Ischemic Wound Healing. Adv Wound Care 2018;7:299-308. DOI: 10.1089/wound.2017.0775
35. Li Q-C, Li C, Zhang W, et al. Potential Effects of Exosomes and their MicroRNA Carrier on Osteoporosis. Curr Pharm Des 2022;28:899-909. DOI: 10.2174/1381612828666220128104206
36. Vig S, Fernandes MH. Bone Cell Exosomes and Emerging Strategies in Bone Engineering. Biomedicines 2022;10:767. DOI: 10.3390/biomedicines10040767
37. Zhang C. Transcriptional regulation of bone formation by the osteoblast-specific transcription factor Osx. J Orthop Surg Res 2010;5:1-8. DOI: 10.1186/1749-799X-5-37
38. Ogata Y. Bone sialoprotein and its transcriptional regulatory mechanism. J Periodontal Res 2008;43:127-35. DOI: 10.1111/j.1600-0765.2007.01014.x
39. Takeuchi R, Katagiri W, Endo S, et al. Exosomes from conditioned media of bone marrow-derived mesenchymal stem cells promote bone regeneration by enhancing angiogenesis. PLoS One 2019;14:1-19. DOI: 10.1371/journal.pone.0225472
40. Liu W, Li L, Rong Y, et al. Hypoxic mesenchymal stem cell-derived exosomes promote bone fracture healing by the transfer of miR-126. Acta Biomater 2020;103:196-212. DOI: 10.1016/j.actbio.2019.12.020
41. Qin Y, Wang L, Gao Z, et al. Bone marrow stromal/stem cell-derived extracellular vesicles regulate osteoblast activity and differentiation in vitro and promote bone regeneration in vivo. Sci Rep 2016;6:1-11. DOI: 10.1038/srep21961
42. Wang Y, Zhou X, Wang D. Mesenchymal Stem Cell-Derived Extracellular Vesicles Inhibit Osteoporosis via MicroRNA-27a-Induced Inhibition of DKK2-Mediated Wnt/β-Catenin Pathway. Inflammation 2022;45:780-99. DOI: 10.1007/s10753-021-01583-z
43. Hu H, Wang D, Li L, et al. Role of microRNA-335 carried by bone marrow mesenchymal stem cells-derived extracellular vesicles in bone fracture recovery. Cell Death Dis 2021;12:156. DOI: 10.1038/s41419-021-03430-3
44. Hotamisligil GS, Bernlohr DA. Metabolic functions of FABPs - Mechanisms and therapeutic implications. Nat Rev Endocrinol 2015;11:592-605. DOI: 10.1038/nrendo.2015.122